
Development of a 12.4 GHz Bandwidth Frequency Offset Locking Unit for Two-Laser Systems

Author:

Steve NOVAKOV

Supervisor:

Dr. Kirk MADISON

FINAL VERSION

UNIVERSITY OF BRITISH COLUMBIA
QUANTUM DEGENERATE GASES LABORATORY
MADISON GROUP

May 25, 2015

Contents

Glossary of Terms	3
1 Overview	4
2 Theory	6
3 Implementation	8
3.1 Procurement	8
3.2 FO Receiver CCA	9
3.3 Frequency/Phase Discriminator CCA	11
3.4 Power Distribution CCA	11
3.5 Enclosure	12
3.5.1 Mounting Specifics	12
4 Testing	14
4.1 Clock Multiplier Pipeline	14
4.1.1 Power Spectrum Analysis	14
4.1.2 Carrier Power Through Multiplier Pipeline	14
4.2 FO Receiver CCA	16
4.3 FPD CCA	16
4.4 Closed Loop Testing of 9200 – 11800 MHz Unit	17
5 Conclusion	20
Appendix	22
A Remaining Build Tasks (TODO list)	22
B User Guide	24
C Signal Processing Block Diagrams	26
C.1 9200 – 11800 MHz Unit	26
C.2 3400 – 7800 MHz Unit	27
C.3 200 – 4400 MHz Unit	28

Glossary

CCA	Circuit Card Assembly: includes a PBC and all of its components, sometimes includes complimentary mechanical components as well.
DDS	Direct digital synthesizer: a synthesizer used for creating arbitrary waveforms from a reference clock.
EMI	Electromagnetic Interference: two types: radiated and conducted.
FO (Receiver)	Fiber Optic (photosensor unit for detecting fiber optic signals).
FOL	Frequency Offset Lock(ing): a method or device of locking two lasers to a fixed frequency offset, (their difference in frequency is fixed).
FPD	Frequency-Phase Discriminator: a digital device which takes in two square-wave inputs and generates an output that indicates when the two inputs are identical in frequency and are separated by some phase, $\phi \in [0, 2\pi]$.
MOT	Magneto-optical Trap.
PCB	Printed Circuit Board.
PSU	Power supply unit.
RF	Radio Frequency. Used to refer to components or systems which operate in the 3 kHz - 300 GHz regime.
ROSA	Receiver optical sub-assembly
SMPS	Switch-mode Power Supply: a power supply that utilizes energy conversion principles such as buck, boost, buck-boost, etc, typically driven at a particular switching frequency, as per the demands of the application.
VCO	Voltage Controlled Oscillator, may be crystal or PLL based.
V_{PP}	Peak-to-peak voltage: the full range of voltage of a particular waveform.

1 Overview

This document outlines the development of an error-signal generating unit for a control system which ensures that two lasers maintain a fixed frequency offset (referred to as “FOL unit”). The Madison Group of the UBC Quantum Degenerate Gases Laboratory specializes in optical manipulation of ultra-cold atomic gases including ${}^6\text{Li}$ and ${}^{87}\text{Rb}/{}^{85}\text{Rb}$. Specifically, this unit will be used to maintain a system of two lasers that are offset at fixed frequencies ¹. These frequencies may, for example, correspond to distinct energy levels for use in laser cooling applications such as Doppler cooling, evaporative cooling in dipole traps, STIRAP, etc. The Madison Group was previously using a simple frequency offset locking unit for ${}^6\text{Li}$ D2 cooling based on an existing popular design that generated a spectrum of locking points [7]. Unfortunately, this method involves significant human intervention and is not simple to automate. Furthermore, the RF components used in this older design limit the bandwidth to ~ 2.0 GHz. The new FOL units should ideally isolate a single null lock point for any subsequent control system to lock to and have a much higher bandwidth.

The intended use of this particular set of FOL units is to fix groups of lasers to desirable frequencies for Doppler Cooling of ${}^6\text{Li}$ and ${}^{87}\text{Rb}/{}^{85}\text{Rb}$ in an “optical molasses”-type MOT. The cooling process involves optically stimulating a trapped gas to undergo a two-state transition in such a way that it loses kinetic energy ². To achieve efficient cooling, the cooling lasers (different from trapping lasers) must be tuned to specific atomic transitions to maximize the absorption and stimulated emission between the target states, and to increase the directional specificity of the cooling action. Depending on the atomic species in use, this frequency offset ranges widely. As an example, for ${}^{40}\text{K}$ D1 Doppler cooling the offset frequency might be ≈ 1 GHz, while for ${}^6\text{Li}$, the D1-D2 separation is ≈ 10 GHz [1, 6, 8, 9, 3].

This FOL unit incorporates a high speed fiber-optic receiver that mixes the two pumping lasers and transmits a waveform with the frequency of the two lasers’ beat-note. This signal is then further processed and mixed until, finally, it is compared to a precision reference that allows locking to a single null lock point. The Madison Group requires FOL units to maintain the following frequency offsets, for use in ${}^6\text{Li}$, ${}^{87}\text{Rb}$ and ${}^{85}\text{Rb}$ experiments [8, 9, 3]:

- ${}^6\text{Li}$ D1-D2 separation : 10.056 GHz
- ${}^{87}\text{Rb}$ D2 pump/repump separation : 6.568 GHz
- ${}^{85}\text{Rb}$ D2 pump/repump separation : 2.915 GHz

Alternately, for the Rubidium experiments, it may be prudent to link both ${}^{87}\text{Rb}$ and ${}^{85}\text{Rb}$ beam sets to a single master laser (for example, the ${}^{87}\text{Rb}$ pump beam). In this case, 3 offset locks could be used for the following couplings:

- ${}^{87}\text{Rb}$ D2 pump - ${}^{87}\text{Rb}$ D2 repump = 6.568 GHz
- ${}^{87}\text{Rb}$ D2 pump - ${}^{85}\text{Rb}$ D2 repump = 4.041 GHz
- ${}^{87}\text{Rb}$ D2 pump - ${}^{85}\text{Rb}$ D2 pump = 1.126 GHz

Regardless of which locking scheme is desired, the FOL units can be reconfigured to function for any offsets up to 12-13 GHz, where the bandwidth becomes limited by the fiber optic receiver, the 4x VCO multiplier pipeline and also cabling.

¹systems of more than two lasers simply require multiple FOL units

²This statement is simplistic, but the nuances of the trapping mechanism are not relevant here.

Three FOL units were assembled, through only one was completed and fully tested. The frequency offset ranges for each of the three units is as follows:

- 9200 – 11800 MHz
- 3400 – 7800 MHz
- 200 – 4400 MHz

The 9200 – 11800 MHz FOL unit was tested in closed loop operation and was found to function as desired. The unit was successfully used to lock two lasers (λ approx. 780nm) to a stable offset, with no visible impact to the linewidth of the laser beatnote between closed and open loop operation. The 200-4400 MHz and 3400-7800 MHz units are currently incomplete and require further assembly as specific components were not available at the time of this writing. Remaining assembly tasks are outlined in **Appendix A**. All relevant design files, including schematics, PCB layout and Bill of Materials for all items (including the enclosure itself) are contained in the archive of work transferred to the Madison Group at project completion. ³ Instructions on how to user these units are provided in **Appendix B**.

³ Concise collections of relevant material, intended for those not wishing to analyze or change design fundamentals, can be found in the <root>/Reports/Summer 2014 Completion Report/. Detailed design files, such as PCB layout, specific calculations, etc, can be found in <root>/D1 Cooling/Locking Amp Upgrade/

2 Theory

The primary input control signal of the FOL units is two fiber-coupled laser beams, with frequencies ω_1 and ω_2 . The two beams are then sent into a fiber optic receiver. The output current of the internal photosensor is dependent on incident power:

$$I_{out} \propto P_{sense} = |\vec{E}_1 + \vec{E}_2|^2 = E_1^2 + E_2^2 + 2E_1E_2 \cos((\omega_1 - \omega_2)t) \quad (1)$$

where $\nu_B = |\omega_1 - \omega_2|$, the beat-note frequency, is the frequency offset that is to be controlled. Minimal interference is assumed and the profile of the beam modes is ignored. The photosensor is AC-coupled to its transmission line(s) and so only the AC signal with the beat-note frequency propagates into subsequent electronics.

To lock to a desired frequency offset, ν_{DO} , the signal is passively mixed with a reference oscillator with frequency ν_{VCO} . This generates a new signal:

$$I_{MIX} \propto (\cos((\nu_B + \nu_{VCO})t) + \cos((\nu_B - \nu_{VCO})t)) \quad (2)$$

At this stage, if $\nu_{VCO} = \nu_{DO}$, one can pass this signal through an LPF to eliminate the high frequency term, and mix it with a phase delayed version of itself to generate the following spectrum [7]:

$$I_{MIX} \propto \cos((\nu_B - \nu_{VCO})2\pi c/L) \quad (3)$$

where the term $2\pi c/L$ is a relation for the phase shift added as a function of delay cable length. however, this generates an infinite spectrum of lock points, specifically when:

$$\nu_B = \frac{nL}{c} + \nu_{VCO} \quad | \quad n \in \mathbb{Z} \quad (4)$$

making it extremely difficult to utilize a controller which can automatically lock to a single lock point without substantial human intervention. It is easy to imagine extending this principle to couple to some external feedback from the sample itself, such as the fluorescent response of a product species, and *then* use that information to cycle between lock points. However, there is a more economical method to extend this principle of “beatnote mixing” to create a system which locks to a single lock point.

In this regard, an alternate approach was chosen: the use of a Frequency-Phase Discriminator (FPD) unit, specifically AD9901 from Analog Devices. This device functions is that it generates a square wave output that is triggered by the rising edges of two input waveforms (can be configured for either TTL or ECL logic) : detection of edge one turns the output on and detection of edge two turns the output off until edge one is detected again, etc. Essentially, the FPD unit outputs a signal that is modulated according to accumulated phase error between the two inputs. If the two input signals have significantly different frequencies, the phase error will accumulate quickly, and the rectified, filtered output will tend towards one of the voltage rails. Similarly, if the two input signals are identical in frequency, but have a phase offset near $\phi = 0$ or $\phi = 2\pi$, a similar output will occur. **Figure 1** shows a visualization of this process; for a more detailed overview, consult the component datasheet [2]. The laser PID controller will servo the laser beatnote until the FPD generates a zero output. However, because the FPD requires two square wave inputs, it is not correct to set ν_{VCO} to ν_{DO} . Instead, if a reference signal, from, for example,

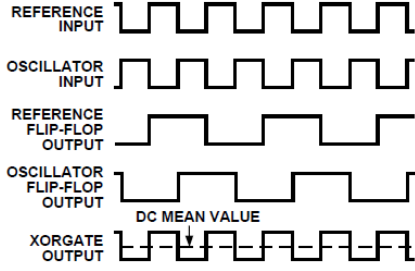


Figure 4. AD9901 Timing Waveforms at "Lock"

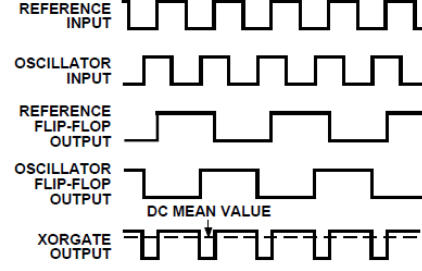


Figure 5. Timing Waveforms (ϕ_{OUT} Leads ϕ_{IN})

Figure 1: I/O summary of AD9901 with varying phase offsets for two inputs very close in frequency. Borrowed from component datasheet [2].

an existing DDS unit, is supplied with a frequency ν_{DDS} , then, for ν_B to lock to ν_{DO} :

$$\nu_{VCO} = \nu_{DO} - \nu_{DDS} \quad (5)$$

where ν_{DDS} is some frequency inside of the FPD circuit's bandwidth, (presumably near the center). This pipeline creates the error signal shown in **Figure 2**. The actual response profile is subject to variation among devices, specifically the slope around the lock points, and so a qualitative description is presented. This behaviour is useful because, outside of a small excursion from $\Delta\phi = \pm\pi$, the filtered output tends away from 0 VDC. While there are still two lock-points instead of, ideally, one (at ν_{DO} and $\nu_{DO} + 2\nu_{DDS}$)

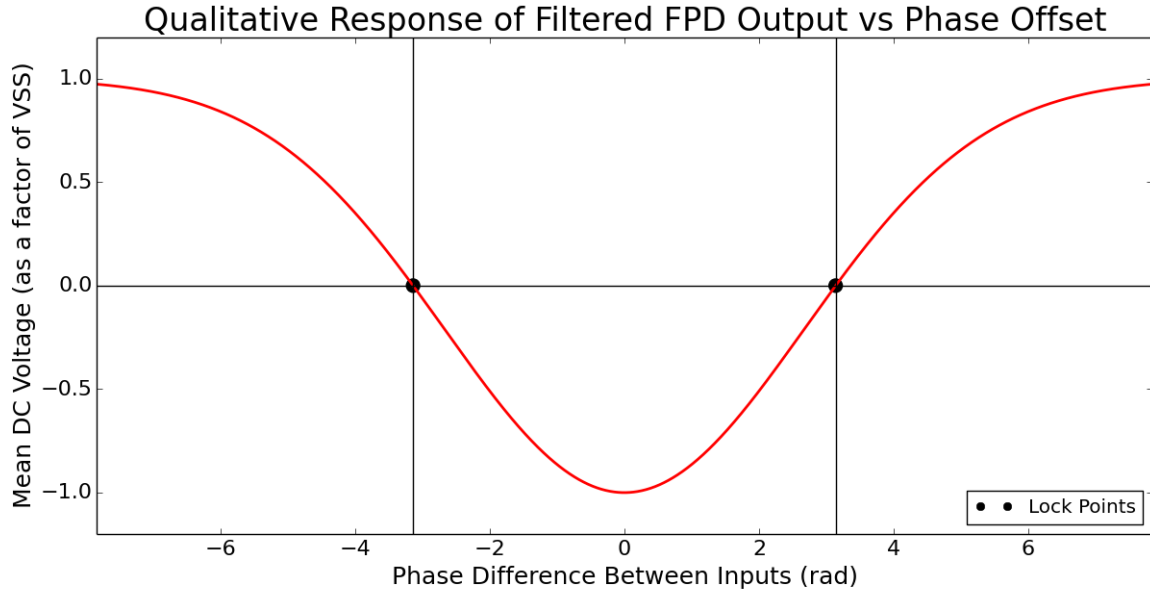


Figure 2: Qualitative description of the output response of a zero-centered, low pass filtered AD9901 output with two identical frequency inputs that have a specific phase difference. The absolute difference is dictated by the phase separation of the "clock" input from the "reference" input.

it is trivial to identify which lock point has been reached by briefly modulating ν_B and observing whether the output servo signal is in-phase (ν_{DO}) or out of phase by $\pm\pi$ ($\nu_{DO} + 2\nu_{DDS}$). Also, this method makes changing ν_B easier, as one can tune ν_{VCO} to some optimal setting and then vary ν_{DDS} as desired. Varying ν_{DDS} is preferred (as opposed to ν_{VCO}) as they are connected to the laboratory ethernet and the Madison Group has Python-based scripts to control them from any desired workstation.

3 Implementation

The frequency offset locking unit developed here is based around a collection of discrete RF components from MiniCircuits, a clock generator development kit from Analog Devices (ADF4350) and several custom PCB's for signal processing and power distribution. The unit mixes the beatnote of two lasers to the reference VCO and extracts the phase error, as explained in **Section 2**. Essentially the device uses the same setup as that in [7], but replaces the cable-delay mixing scheme with a frequency-phase discriminator unit, which reduces the number lock points to one, and alleviates the need for human intervention. Three FOL units were assembled, though only the unit for the ${}^6\text{Li}$ D1-D2 (10.056 GHz) unit was completed and tested in closed loop operation. It is intended that all FOL enclosures are controlled by a single FPGA-based controller, currently in development. For a detailed block diagram, including power distribution info, of all three FOL units, see **Figures 7, 8** and **Appendix C.1 – C.3**.

All components share the same ground reference, which is also tied to the enclosure chassis. The units were designed to be powered by the UBC QDG lab standard power supplies, using only the $\pm 5.0\text{V}$ and $+15.0\text{V}$ rails. Unless the input power supply is especially noisy, this should not result in excessive radiated EMI, as all high-speed transmission lines have tight return paths. If it is noticed that turning these units on induces noise in other equipment, for example, then it may be sufficient to replace the metal standoffs, for the various CCA's and discrete RF components, with plastic ones. To reduce phase noise, it is intended that both the ADF4350 reference input for the VCO pipeline and the DDS output for the FPD CCA reference are GPS stabilized. Three new CCAs were designed to support the following:

- Power distribution
- HFD6180 LC ROSA photo-sensor
- AD9901 Frequency Phase Discriminator

The HFD6180 photo-sensor unit, manufactured by Finisar, has been in frequent use at the Madison Lab, based in a portable, stand-alone enclosure. With a reported bandwidth of 12GHz, the unit is well suited for use with various Li, Rb experiments which have transitions/offsets in the 1-11GHz range [3, 8, 9]. The AD9901 FPD unit has also been used previously, in a larger FPD unit designed by the UBC Physics ELAB (E06-012-01). This unit included substantial electronics for on-board manipulation of the indecent reference waveform. While this board could have potentially been re-purposed for this FOL unit, it was not functionally useful: it has excessive connectors/components and the connectors are awkwardly placed. Additionally, there was only one spare E06-012-01 at the time of writing, and commissioning three more full enclosures was deemed excessive. To eliminate the unnecessary components, a much smaller CCA was designed to include only the necessary supporting electronics for AD9901, to the exclusion of all else. Lastly, a simple power-distribution CCA was designed to regulate $+12\text{V}$ and feed/filter the $\pm 5.0\text{V}$ rails to various components was designed, to ease installation and debugging.

3.1 Procurement

The CCAs were designed in-house using Altium Designer software and were manufactured by Alberta Printed Circuits on two-layer, 0.062" PCBs ⁴. As mentioned, design files were transferred to the Madison Group upon project completion. With respect to supporting different ranges of frequency offsets, enclosure conversion only entails removal/addition of components in the frequency multiplier chain. It is

⁴www.apcircuits.com

intended that the rest of the components remain fixed in placement and configuration.

The FO receiver CCA, though small in size and sparse of components, does feature the \$50 HFD6180 photosensor, which must be procured in batches of 30 from the manufacturer, Finisar (can purchase through Mouser Electronics). All other surface mount components, cables and connectors were purchased from Digi-key and Newark ⁵. Discrete RF modules, specifically filters, amplifiers, mixers and frequency doublers, are acquired from Mini-Circuits and linked together with co-axial cables with SMA connectors. **Table 1** gives a cost breakdown of the entire FOL unit, by major subunits.

Component(s)	Sub-component(s)	Cost
FO Receiver CCA	PCB Components	\$70
	PCB	\$20
FPD CCA	PCB Components	\$160
	PCB	\$55
PWR CCA	PCB Components	\$5
	PCB	\$35
Enclosure, asst	Enclosure Box	\$90
	ADF4350EVAL Kit	\$180
	Panel Connectors	\$40
	Mounting Hardware	\$15
	Incidental Items	\$200
RF Components & Cabling	RF Components (full multi)	\$550 (\$1100)
	Cabling (full multi)	\$100 (\$180)
Total (full multi)		\$1600 (\$2200)

Table 1: Component cost for enclosure. The term “full multi” refers to the configuration with the full 2x multiplier stage for the VCO. “Incidental Items” includes such things as wiring, WaterJet time, etc.

3.2 FO Receiver CCA

Previously, the Madison Group contracted the UBC Physics department’s Electronics Lab to design a standalone FO receiver unit for use in experiments and calibrations. This design, part number E06-029-01, was created in two variants: a simple version that just feeds the HFD6180 output to an SMA connector, and a downscaling-capable version that enables dividing down the receiver output 16x. Unfortunately, this functionality was not often used, and because the designs shared the same PCB (one simply has the divide-down components unpopulated), this means that the existing boards are unnecessarily large and have suboptimal transmission lines to the SMA connector. E06-029-01 demanded a redesign for two reasons: maximizing the output power of the ν_B carrier, and reducing size so that the new FO receiver units were as small as possible. Attenuation can be reduced by a straight, impedance controlled trace from the receiver to the connector. A smaller board/enclosure ensures a shorter trace length and is generally easier to maneuver and position in and around optical assemblies. The new CCA, populated and with its fiber adaptor is shown in **Figure 3**.

The new design, E06-029-02, removed any superfluous components directly unrelated to operation of HFD6180 and reduced the board size by about one half. The mechanical interface, holding the HFD6180 receiver and aligning it with an LC fiber connector, comes in two pieces: the connector itself, and a locking wedge to ensure proper alignment and prevent movement. In earlier testing, with the E06-029-01 CCA, the HFD6180 was shown to output a beatnote signal with power > -40 dBm up to 16GHz [5]. As

⁵The Madison Group has a contact at Newark that compiles BOMs and applies CFI discounts, please ask lab staff for specifics.

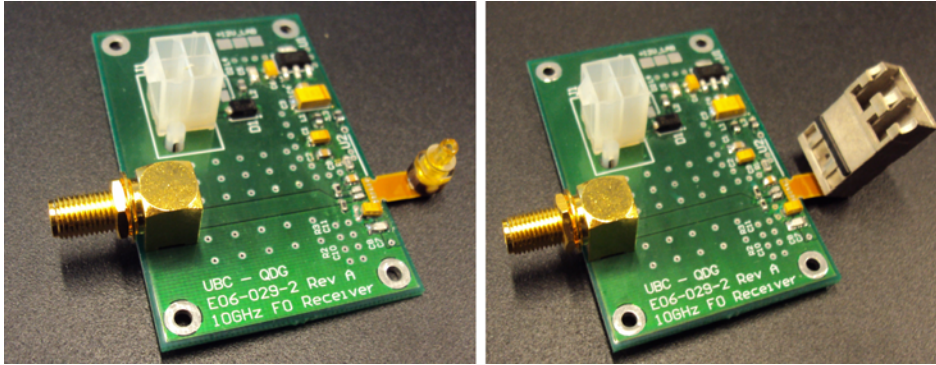


Figure 3: FO receiver CCA, QDG-E06-029-02, with (right) and without (left) LC fiber adaptor.

will be shown, this new CCA puts out a higher power signal at comparable frequencies, and, therefore, a slightly higher useable bandwidth can be expected.

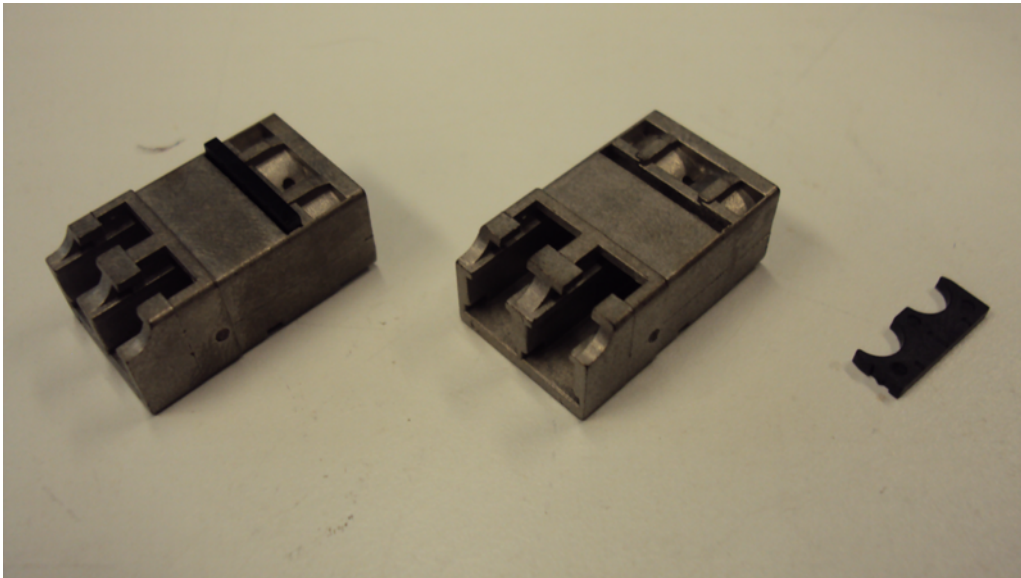


Figure 4: MicroPEP LC Transciever Housing, with locking wedge, inserted (left) and not (right).

3.3 Frequency/Phase Discriminator CCA

The new FPD CCA is a re-factoring of an existing unit built by the PHAS Electronics Lab, E06-012-01. E06-012-01 is likely based off of an earlier design by JILA labs, which features both the AD9901 and an on-board MCU/VCO [4]. There are many DDS units in the Madison Labs, and it is intended that some of them be (re)purposed to serve as reference inputs for the FPD CCAs in each enclosure. It is expected that these DDS units are also GPS stabilized. The FPD CCA has three main stages:

- **Input Comparators + ECL logic conversion** - The two input signals are processed by comparators with $\sim 0.350V$ hysteresis, centered on GND. These are then converted to NECL logic with NECL NOR gates.
- **AD9901** - The AD9901 is configured in NECL mode.
- **Rectifier, Filter and Servo Signal** - The AD9901 signal is then filtered to extract the mean DC value, in the range $\pm 5.0V$ and is filtered for processing (peak follower filter). There are two, buffered, output signals, a “phase monitor” which is the raw output, and the “servo” output, which is manually scaled in amplitude with a potentiometer and is to be connected to the laser PI servo.

The input comparator stage has a bandwidth of 200 MHz, limited by the input comparators and the AD9901 itself. This is more than sufficient as the DDS units in the QDG lab only have a bandwidth of 135 MHz. The output filter stage is, by default, configured to have a maximum bandwidth of 1 MHz. This provides the maximum amount of filtering while not limiting the laser servo controller, which has a bandwidth in the same range. Changing this value is simple and only involves modifying passive filter components on the CCA. **The input comparators expect inputs of, at minimum, 400 mVpp to function correctly.** ⁶

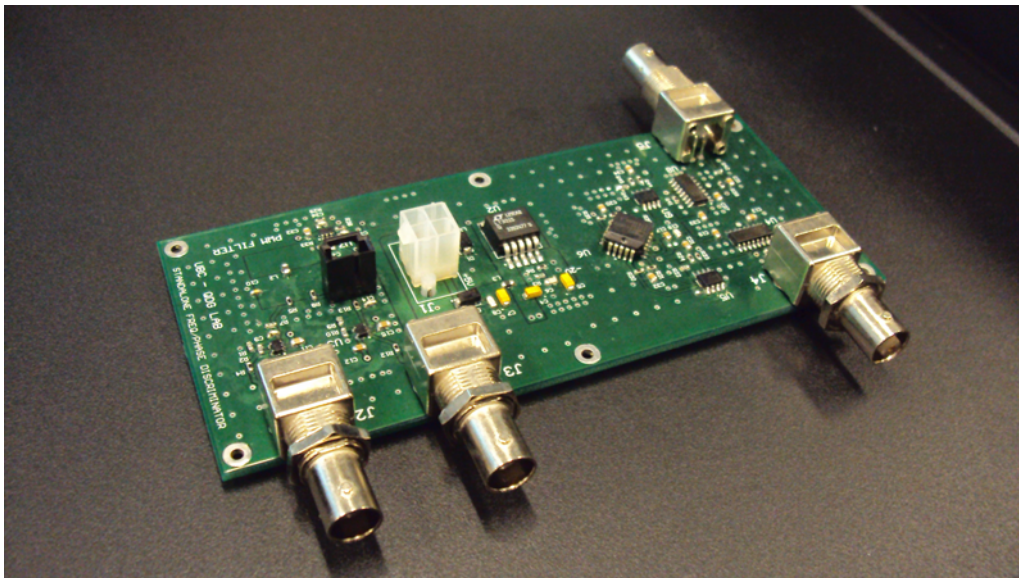


Figure 5: FPD CCA, shown from the panel mounting side.

3.4 Power Distribution CCA

A simple connector board was created to neatly supply power to the various RF components and CCAs. Only the FPD board uses the $-5.0V$ rail and all discrete RF components use $+12.0V$ or $+5.0V$. The

⁶For closed loop testing of the 9200 – 11800 MHz unit, the error signal coming out of the final mixer/amplifiers had an amplitude of approximately 1.8-2.0 Vpp, or +9-10 dBm.

+12.0V rail is generated with an LDO from the +15.0V QDG Lab Power rail. Initially, it was thought that it would be sufficient to simply feedforward the QDG Lab Power $\pm 5.0V$ rails to the various CCAs and components and that the wire resistance, estimated at $\sim 0.3\Omega$ total would not drop the rails below required levels. Unfortunately, many components require +5.0V and it is not possible to use an LDO to regulate to +3.3V, for example. It is possible that, with longer power cables, these rails might drop to levels below the threshold required for digital components to function correctly, so care must be taken during installation. Though it would provide more stable supply voltages, it was specified by the QDG lab staff that using on-board SMPS components is not desirable, as the QDG Lab Power Supplies power various sensitive instrumentation, which any conducted EMI may disrupt.

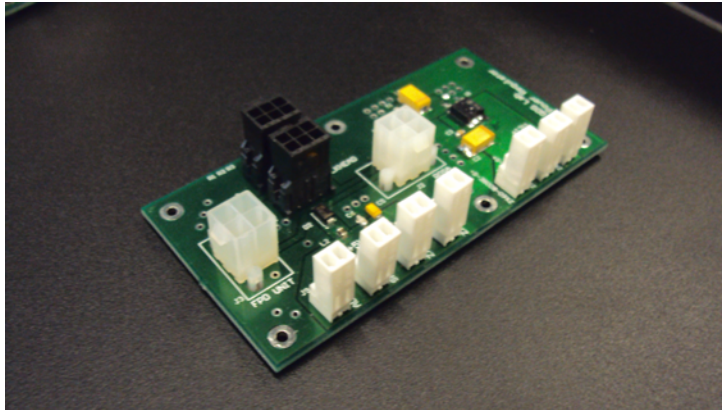


Figure 6: Power Distribution CCA, with 2 pin connectors for RF amplifiers, 4 pin connectors for the FPD and FO Receiver CCAs and 6 pin connectors for the PSU and indicator LEDs.

3.5 Enclosure

For simplicity, a stock 1u (standard rack unit: 1.75" tall) enclosure ⁷ was purchased that would sufficiently contain any variant of the FOL unit. The front, rear and floor panels of the enclosure were cut with the Hebb 42 WaterJet machine. While purchasing a stock enclosure does save some manufacturing time, it is still quite difficult to ensure alignment for particular sub-components as consistency between WaterJet cuts of these (rather small and thin) components is difficult. Fortunately, there is sufficient space for various manual adjustments. All discrete RF components, and PCBs are attached to the floor. The FPD and FO receiver CCAs have a second attachment to the front and rear panels, respectively. The populated 9200 – 11800 MHz FOL unit is pictured in **Figure 7** and a corresponding connectivity diagram is shown in **Figure 8**. The only difference between the three FOL unit builds is the type and number of RF components in the signal processing pipeline. The three variations are shown in **Appendices C.2 – C.3**.

3.5.1 Mounting Specifics

Ensuring that the floor holes of the FPD and FO receiver CCAs align with their front and rear panel cutouts is quite difficult. To compensate for this, the front/rear panel cutouts were cut with the WaterJet machine and that the floor holes for these CCAs were later hand drilled. Special care was taken when mounting the FO receiver CCA. Because the photosensor is connected to the CCA with a rigid-flex PCB, it is important to reduce the strain on it as much as possible. The transceiver housing, unfortunately, is not manufactured with mounting flanges and must be secured to the rear panel with either some sort of clamping mount, or with epoxy, which was chosen due to time constraints.

⁷RMCS190113BK1

4 Testing

All CCAs underwent basic electrical testing: ensuring the correct net connectivity, no short-circuit conditions, correct voltage levels on power supply rails, etc. Additionally, the highest bandwidth unit, for ${}^6\text{Li}$ D1-D2 locking, underwent closed loop testing with a laser servo controller with PI feedback.

4.1 Clock Multiplier Pipeline

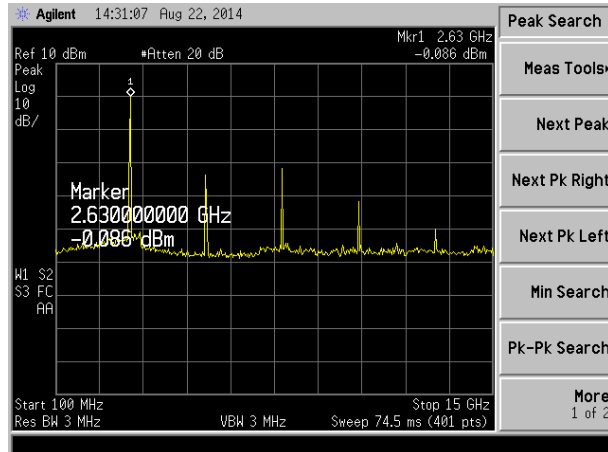
Throughout the pipeline, it is important that the carrier power is as expected during the design stage. If the carrier power is insufficient, then the amplitude of the VCO signal coming into the FPD CCA will be insufficient to properly trigger the input comparators, rendering it invisible. Without additional amplifiers, the carrier power coming out of the full 4x multiplier pipeline for the ADF4350 seems to be significantly lower than expected, by ~ 5 dB consistently. With respect to the signals' power spectra, it is important that the fundamental of any signals that are to be mixed with the laser beat-note does not have nearby side-bands of significant amplitude. If there are, for example, two or more mixing stages, it is highly likely that the final signal will have multiple, high amplitude frequency components, rather than one predominant carrier. In these conditions, upon mixing with the laser beat-note, it is likely that there will be more than one set of valid lock points. If the varied frequency offset starts significantly far away from the desired lock point, it will not be possible for an automated system to lock to this value, as it will have no distinction between any available sets of lock points.

4.1.1 Power Spectrum Analysis

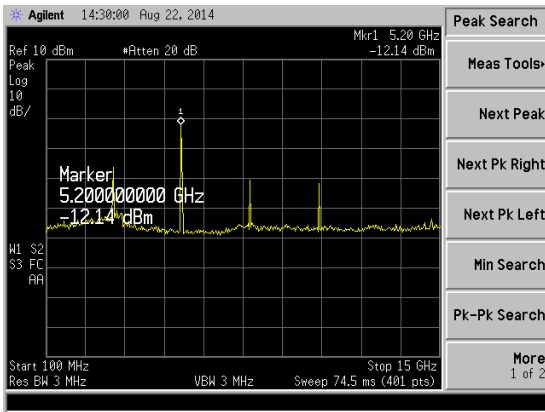
Using the in-house Agilent E4407B (25.6 GHz bandwidth), measurements of the power spectrum of the signal were taken at every stage of the full VCO multiplier pipeline, for use in the ${}^6\text{Li}$ D1-D2 locking. **Figure 9** shows the raw output at every relevant step. From the distinct fourier series shown in the first picture, it is evident that the ADF4350 is generating a waveform that is mostly a square wave, around the fundamental of 2.63 GHz. However, upon mixing in the first passive frequency doubler, it is evident that the side-bands are brought closer to the carrier, in terms of relative power. Further amplification seems to bring the carrier and side-bands even closer in power, from -30 dBc at the clock generator, to ~ -10 -15 dBc at the final stage. If the VCO signal sideband amplitudes are significant, it is possible that the offset locking will occur for one of these sidebands rather than the desired carrier. However, as these sidebands are a product of the VCO mixing with itself in the passive frequency multiplication electronics, their separation is always an integer multiple of the fundamental. In the case of the 4x pipeline, this fundamental is ~ 2.5 GHz, which is large. The locking process itself involves manually bringing ν_B to within 1 – 300 MHz of ν_{VCO} , so it is unlikely that a human operator would mistake one of the sidebands for the carrier.

4.1.2 Carrier Power Through Multiplier Pipeline

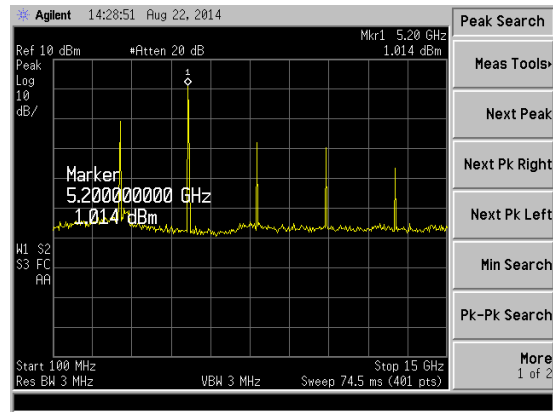
The input comparators, in the original design, have trigger voltages of -174mV and 145mV. Assuming 50 Ω termination, this demands a carrier with approximately 8dBm of input power, which is slightly less than the *expected* power out of the mixing circuit. The DDS units will have no problem supplying this. Unfortunately, it seems as though there is quite a bit of variance in the gain/conversion loss of the MiniCircuits discrete modules and the VCO carrier in the ${}^6\text{Li}$ D1-D2 FOL unit has almost half of the expected power. The waveform was not measured with an oscilloscope due to time constraints, but it is important to verify the input to the FPD has the required amplitude otherwise the AD9901 will hold its output low. In the tested ${}^6\text{Li}$ D1-D2 FOL unit, four *additional* ZX60-43-S+ amplifiers were placed on the output of the passive mixer to bring the carrier past 1 Vpp.



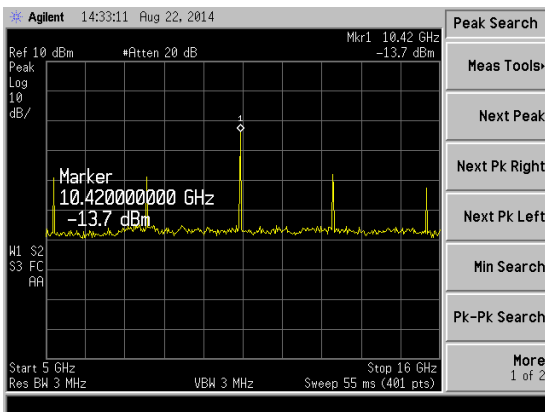
(a) Raw output of ADF4350 (RF_{out+} , specifically, with the other output having a 50Ω terminator), (approx. 1.5GHz/div)



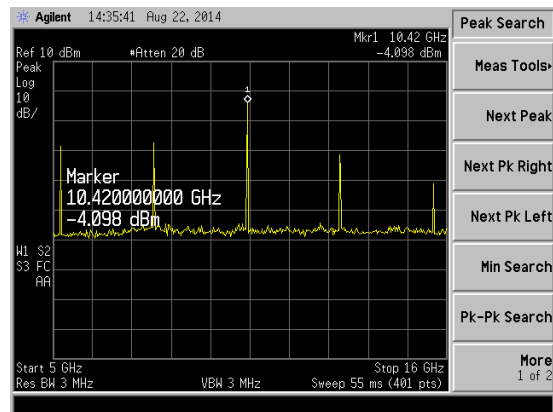
(b) Clock signal after ZX90-2-36-S+, (approx. 1.5GHz/div)



(c) Clock signal after 2x ZX60-8008E-S+, (approx. 1.5GHz/div)



(d) Clock signal after ZX90-2-24-S+, (approx. 1.6GHz/div)



(e) Clock signal after 1x ZX60-14012L-S+, (approx. 1.6GHz/div)

Figure 9: Power spectrum analysis of VCO output at every major step in the Li D1-D2 multiplier pipeline. While sidebands in the final clock signal are significantly lower in power than the carrier, it may be prudent to add an output bandpass filter around the carrier frequency to prevent potential mis-locks. The composition of the signals is as expected, though, it is clear that more mixing steps result in the closing of the power gap between the carrier and the sidebands.

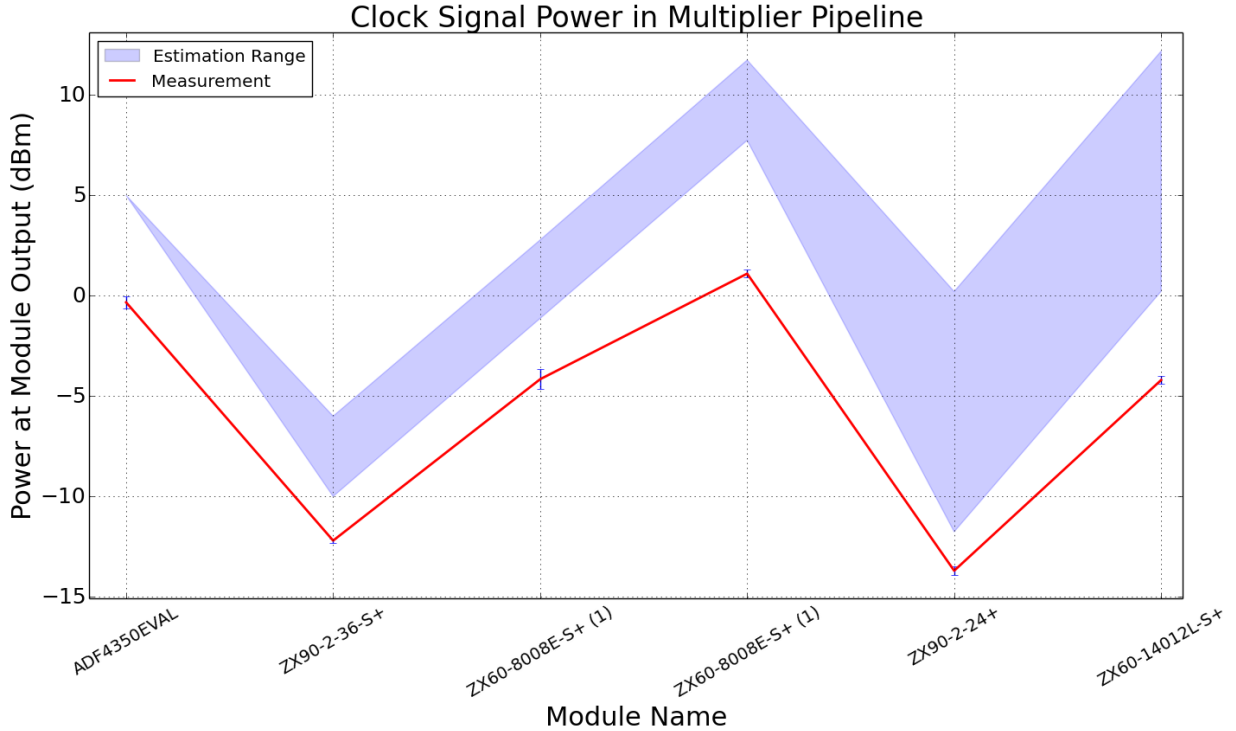


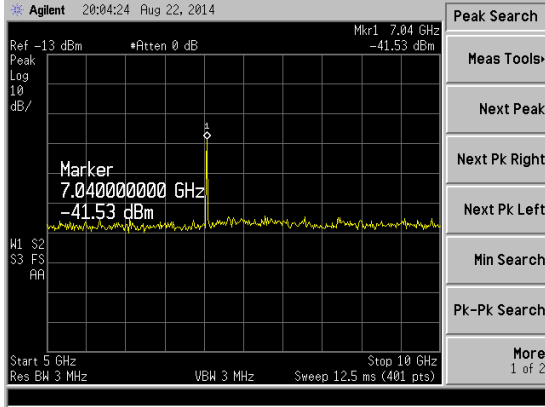
Figure 10: Expected range of carrier powers after a particular multiplier stage (blue) compared with measured powers (red). The possibility of a particular unit being on the low-end of the estimation range was accounted for, with the solution being to simply add another amplifier stage at the end (ZX60-14012L-S+). Unfortunately, to obtain the desired V_{pp} for the final signal, at least two more amplifier stages are required, as the passive mixers drop the carrier power substantially.

4.2 FO Receiver CCA

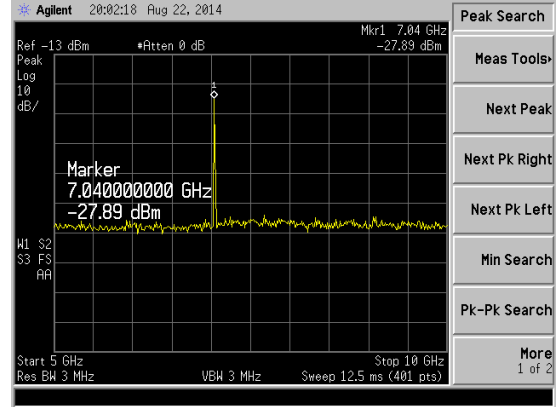
The new photosensor CCA, E06-029-02, was tested against the existing E06-029-01 with identical inputs to compare the overall power spectrum and carrier power of the resultant output. From a preliminary overview, it is expected that E06-029-02 will perform slightly better than E06-029-01 because the transmission line from HFD6180 is more tightly controlled. E06-029-01 has an optional 16x divide-down stage in series with the photo-transistor. In the variants without this stage, the relevant components were removed and the traces from the HFD6180 output were directly soldered to a coaxial cable. In comparison, E06-029-02 has a straight, 50Ω controlled impedance trace directly into an SMA connector, which should result in less attenuation. Comparing the carrier powers in **Figure 11** and **Figure 12**, this seems to hold true. Both figures show tests where the power of both incident lasers were constant between the two variants. The sensor itself was characterized in an earlier investigation [5].

4.3 FPD CCA

The new standalone Frequency/Phase Discriminator CCA was found to have an incorrect footprint for the AD9901 component during testing. During layout, the footprints for the ECL and TTL configurations were accidentally swapped. Through salvaging was attempted via deadbugging (flipping the chip upside down and connecting pins to pads via wires), this was unfruitful and a respin of the CCA was required. During debugging the comparators were found to work as expected, putting out the correct ECL logic levels during operation. The peak-follower and level shifting amplifiers were also found to function correctly. These subcircuits were tested using a function generator and the relevant input waveforms. The respun CCA, with the correct ECL configuration footprint, was recently ordered and will have to be

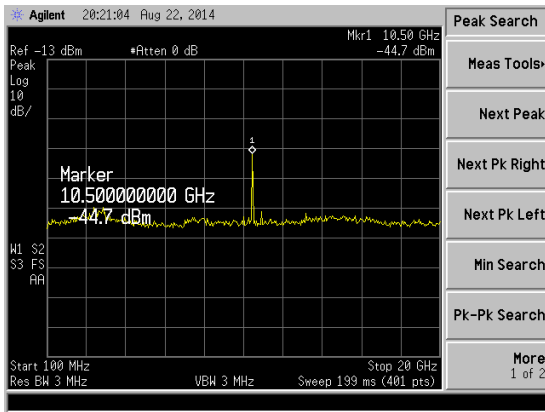


(a) E06-029-01

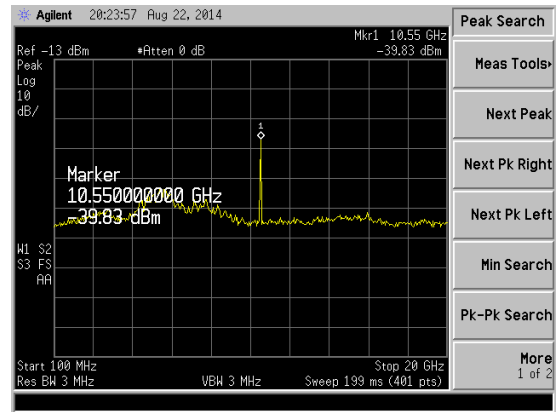


(b) E06-029-02

Figure 11: Comparison of beatnote output power (from an identical source) of E06-029-01/02 at ~ 7 GHz ν_B .



(a) E06-029-01



(b) E06-029-02

Figure 12: Comparison of beatnote output power (from an identical source) of E06-029-01/02 at ~ 10.5 GHz ν_B .

installed and tested at a future date.

4.4 Closed Loop Testing of 9200 – 11800 MHz Unit

In lieu of a working FPD CCA, the otherwise completed 9200 – 11800 MHz FOL unit was connected to a spare E06-012-01 unit (the only one remaining) and underwent closed-loop testing. The two lasers used for testing were both approximately 780 nm wavelength, with one being locked to a resonance of a Rubidium vapour cell. The other laser was first controlled open-loop with an existing laser servo PI controller, before being connected to the FOL unit in a closed-loop configuration.

It was possible to see both the ROSA beatnote signal and the final VCO signal through the ROSA MONITOR output of the enclosure, as the VCO weakly couples through the passive components. The VCO frequency was first set to 11300 MHz and the second laser was manually tuned so that the beatnote was within 100 – 300 MHz of the VCO signal, as shown in **Figure 13**. Then, the mixed error signal and a 120 MHz DDS clock were sent to a E06-012-01 unit, and the output was sent to the error signal input of the laser servo PI controller. The proportional gain was then turned on, and the frequency was changed to 11300 MHz. The beatnote locked to 120 MHz offset from the VCO as shown in **Figure 14a**

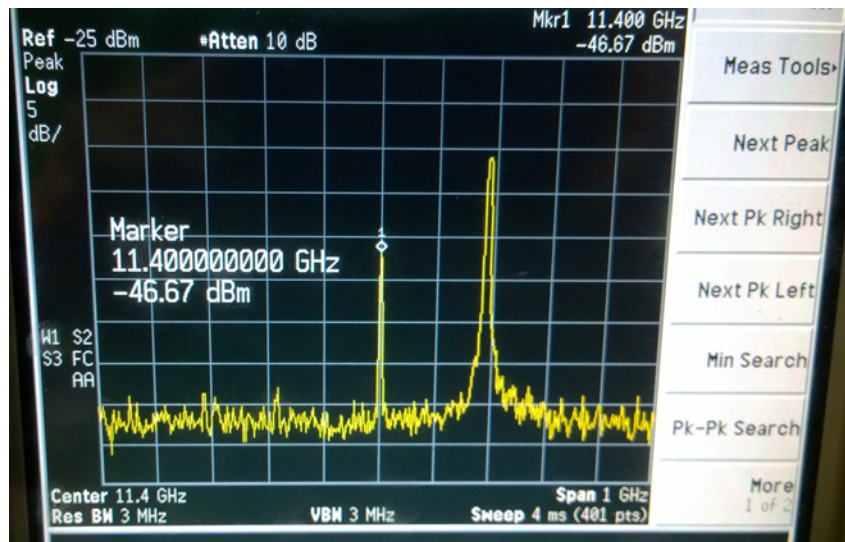
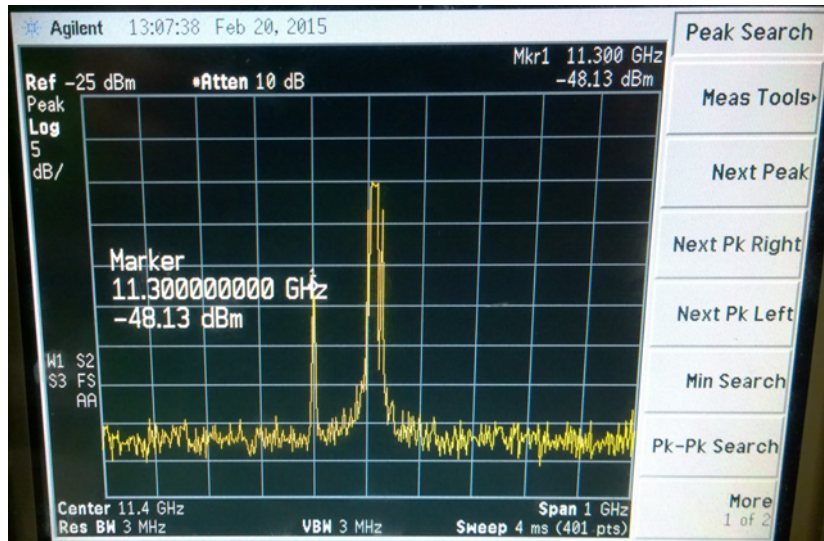
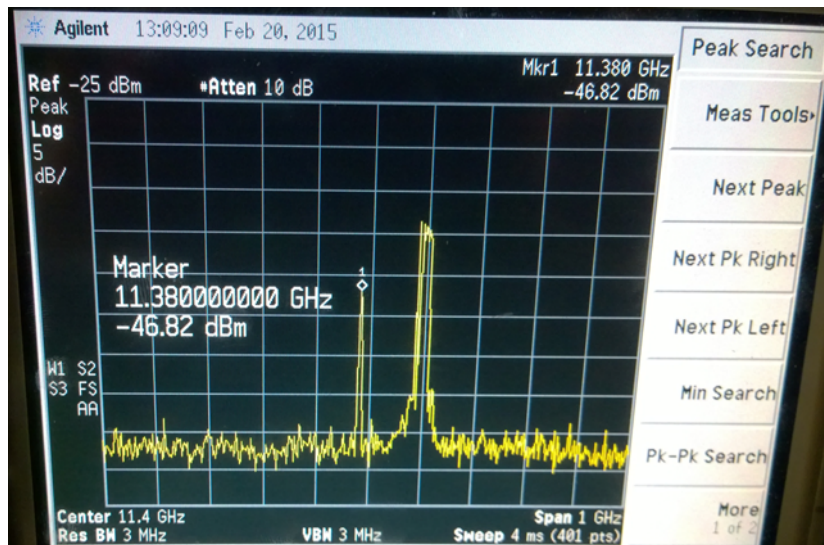


Figure 13: Laser beatnote (right) manually moved to the vicinity of the VCO carrier (center) at 11400 GHz, as sampled at the ROSA MONITOR output. Here the laser servo is turned off, and the beatnote constantly moves around up to several divisions.

and did not change as the VCO was increased to 11380 MHz, as shown in **Figure 14b**. Compared to the beatnote in **Figure 13**, the beatnote linewidth approximately doubles with just proportional gain turned on. This can be corrected by turning on the integral gain and adjusting it. During testing a lock was achieved that had negligible impact on the beatnote linewidth, though that data is not present here. It is expected that these high bandwidth FOL units have less of an impact on the beatnote linewidth (how tightly the second laser is locked to a particular offset) than the servo controller itself, which only has a bandwidth of ~ 1 MHz. Changing the VCO frequency such that it jumps through the beatnote frequency (for example, changing the VCO in **Figure 14a** to 11420 MHz or higher) destroys the lock. During closed loop operation it is not recommended that the user change the locking frequency by more than half the DDS reference clock frequency. However, common tuning is unlikely to exceed MHz, and possibly even kHz of change, so this should not be an issue in regular operation.



(a)



(b)

Figure 14: Closed loop locking to $\nu_{VCO} = 11300$ MHz (a), and 11380 MHz (b), with the laser servo using only proportional gain, as sampled at the ROSA MONITOR output. The resultant laser beatnote is shown on the right in both images. The system was prepared as shown in **Figure 13**, then the servo was turned on. A DDS frequency of 120 MHz was used for the FPD VCO input (hence the offset). Image (b) shows what happens when the system starts locked in the state shown in (a) and a user changes the VCO frequency through a software interface (in this case, by increasing it in software by 20MHz (4x multiplier), such that ν_{VCO} increases by 80 MHz). The system immediately shifts over and stays locked without problems. Unlike in **Figure 13**, the beatnote is essentially confined to the envelope shown. Note the slight “smearing effect”: excessive overshoot can be corrected by turning on the integral gain (not shown here due to lack of images).

5 Conclusion

Three frequency-offset locking units were built for generating error signals for a laser servo PI controller. These units mix the beatnote of two lasers with a reference oscillator to generate an error signal used to lock the carrier frequency of a one laser to a stable offset in frequency from an independently locked master laser. These units will be used to create systems of two or more lasers that stimulate multiple atomic transitions at once. Here, the FOL units were built for experiments requiring stimulation of the ${}^6\text{Li}$ D1-D2 (10.056 GHz), ${}^{87}\text{Rb}$ D2 pump/repump (6.568 GHz) and ${}^{85}\text{Rb}$ D2 pump/repump (2.915 GHz) transitions. The resulting units can lock two lasers to a frequency offset of 9200 – 11800 MHz, 3400 – 7800 MHz, and 200 – 4400 MHz respectively. The 9200 – 11800 MHz FOL unit was fully completed, but the remaining two FOL units (3400 – 7800 MHz and 200 – 4400 MHz) are currently incomplete and are awaiting component orders to arrive. These units were completed to the point where the only remaining built task is to place and connect discrete RF components, a task which should not take significant effort.

The 9200 – 11800 MHz FOL unit underwent closed loop testing and was found to operate as intended. Two lasers were locked to a separation around 11300 MHz and were stable for the duration of testing. The lock point was changed repeatedly via software and locking was maintained. The linewidth of the locked beatnote is larger by a factor of 2-3 when locking with proportional gain only. Turning on integral gain with the correct settings reduces the linewidth to its open-loop value, which indicates that the laser servo controller is not bandwidth limited by the FOL units, as expected. The FOL unit does require some ad-hoc tuning at the first implementation, mostly with regards to finding optimal PI gain parameters for the laser servo controller. However the new Frequency/Phase Discriminator method is more resilient than the existing cable delay method and, once locked, these FOL units should require minimal interference.

These new FOL units will allow for greater fidelity when modifying laser offsets either before or during experiments. Using the highly responsive DDS units present throughout the lab as a reference input for the FPD stage, it is possible and easy to quickly vary the target frequency by 10s of MHz without re-programming the clock generator. These units will allow for quick adaptation to minute changes in experiment parameters, and, particularly, for a higher degree of automation due to the single, more stable null locking point, and high bandwidth.

Acknowledgements

This project was funded by the UBC Quantum Degenerate Gases laboratory led by Dr. Kirk Madison. Dr. Madison provided direct guidance on theoretical matters and contributed significant physical resources. William Bowden, Gene Polovy, Will Gunton and Mariusz Semczuk of the Madison Group were extremely helpful with design and testing procedures, and with setup of lab equipment. Janelle van Dongen provided significant assistance with the laser control instrumentation and data acquisition. Further thanks goes to Dr. Jim Booth, Koko Yu, Kahan Dare and Kais Jooya for their suggestions and guidance. The UBC Chemistry and Physics Electronics Labs were also very helpful as were the Hennings Machine Shop staff.

References

- [1] A. Burchianti et al. “Efficient all-optical production of large ^6Li quantum gases using D_1 gray-molasses cooling”. In: *ArXiv e-prints* (June 2014). arXiv: 1406.4788 [cond-mat.quant-gas].
- [2] Analog Devices. *Ultrahigh Speed Phase/Frequency Discriminator*. obtained from http://www.analog.com/static/imported-files/data_sheets/AD9901.pdf (2014-06-01). 1999.
- [3] Micheal E. Gehm. “Properties of 6Li ”. Available online at <http://www.physics.ncsu.edu/~jet/tech-docs/pdf/PropertiesOfLi.pdf>. Feb. 2003.
- [4] JILA Electronics Lab. *GHz Laser Synchronizer*. DN: YJ029. Aug. 2008.
- [5] Steve Novakov. “Frequency Response of HFD6180 (LC ROSA)”. UBC QDG Lab - Internal Report, available through QDG lab staff. June 2014.
- [6] D. Rio Fernandes et al. “Sub-Doppler laser cooling of fermionic ^{40}K atoms in three-dimensional gray optical molasses”. In: *EPL (Europhysics Letters)* 100 (Dec. 2012), p. 63001. DOI: 10.1209/0295-5075/100/63001. arXiv: 1210.1310 [cond-mat.quant-gas].
- [7] U. Schunemann et al. “Simple scheme for tunable frequency offset locking of two lasers”. In: *Review of Scientific Instruments* (Jan. 1999).
- [8] Daniel A. Steck. “Rubidium 87 D Line Data”. Available online at <http://steck.us/alkalidata>. Dec. 2010.
- [9] Daniel A. Steck. “Rubidium 87 D Line Data”. Available online at <http://steck.us/alkalidata>. Dec. 2010.

NOTE It was asked that the “Frequency Response of HFD6180 (LC ROSA)” report be attached at the end of this document for convenience. It can be found at the end of the Appendices.

Appendix

A Remaining Build Tasks (TODO list)

The ${}^6\text{Li}$ D1-D2 (10.056 GHz) FOL unit was completely built and tested. During testing of this unit, it was found that the FPD CCA had an incorrect land pattern for the AD9901 chip. This error was corrected, but the re-spun CCAs have not arrived as of this writing. The ${}^6\text{Li}$ D1-D2 FOL unit was verified to work in closed loop configuration with a laser PID servo using an existing external FPD unit. Additionally, during building of this unit, it was discovered that the signal carrier power was significantly lower than expected, and multiple amplifiers were added to the design to ensure operation. This caused a shortage of parts for the other two FOL units, and so, the units are only partially complete. The remaining work involves validating and inserting the re-spun FPD CCA and installing the signal processing pipeline when the additional MiniCircuits amplifiers arrive.

Power supply and connectivity information for signal processing pipelines of the the currently incomplete ${}^{87}\text{Rb}/{}^{85}\text{Rb}$ D2 pump/repump FOL units is shown in **Appendices C.2 – C.3**. The existing ${}^6\text{Li}$ D1-D2 FOL unit layout can be used as a placement guide, as shown in **Figures 7, 8**. These units have their panel interfaces, Power Distribution CCAs and ROSA CCAs already installed. One of the enclosures does not have an EVAL-ADF4350EB1Z unit as it has not yet arrived from Newark. Note that there is a space for the FPD CCA in the bottom right corner which can not be populated by MiniCircuits components (though some *shielded* cabling can pass underneath). All active MiniCircuits components (amplifiers) should be connected to the Power Distribution CCA. It is possible that some components will have to “double up” on a power connector as there are only four +5V and three +12V physical connectors on each CCA. Due to lower-than-expected gain from the MiniCircuits amplifiers, the number of required active components will likely exceed the physical connector count on the Power Distribution CCA. **Amplifiers should be added until the FPD REF signal is greater than 1 Vpp, and preferably, on closer to 2 Vpp, to ensure correct triggering of the digital logic and robust operation.** This is the signal right before the FPD which comes out of the passive mixer. If it is insufficiently amplified, the input comparators on the FPD CCA will not trigger correctly and the error signal will be pulled to -5V.

The first spin of the FPD CCA had incorrect pin placement in the AD9901 footprint. A deadbug fix was attempted, but this failed to yield a working circuit. Subcircuit testing indicated that the input comparators and level shifting amplifier subcircuits worked correctly, so it is expected that the footprint fix will yield working boards. For the ${}^6\text{Li}$ D1-D2 (10.056 GHz) FOL unit testing, an external, previously built FPD unit was used. These units are limited (only one spare remains) and so the FPD CCA was re-spun. Three new CCAs are currently being ordered. These will be assembled either in-house or by the PHAS E-Lab. Once assembled, these need to be installed in all three FOL enclosures, as shown in **Figure 8**. The CCA is to be inserted into the side panel holes for the BNC connectors, and these are to be fastened with the provided hex nuts (they come with the BNC connector). Then, spacers are placed between the mounting holes and the enclosure bottom and then the CCA is bolted in place, as shown here:

Ensure that no other components, with the exception of shielded cabling, are present underneath the FPD CCA after mounting. The potentiometer for scaling the SERVO output can be connected to the CCA as desired, though male/female 0.100" headers are recommended for simplicity. The silkscreen should indicate the correct connection points for the potentiometer, but please consult the schematic first.

NOTE Only use the white SMA cables (for example, 415-0025-006) for circuits with a required bandwidth of 4 GHz or less. The SMA cables with the beige/speckled shielding (such as 135101-01-06.00) may be used for any bandwidth up to 12.4 GHz.

B User Guide

A simple start-up guide is presented here for first time use. Please refer to **Figures 7, 8** for physical orientation.

1. Couple the reference laser and the offset laser into a fiber with an LC connector. Each beam should be in the 200-500 μW range for optimal operation. **Do not exceed 1 mW total input power into the HFD6180 ROSA sensor.** Insert the LC connector into the appropriate port on the rear of the enclosure.
2. Ensure the 5-pin LAB POWER connector is inserted and press the POWER switch on the front of the box. Ensure that all 3 green indicator LED's are lit ($\pm 5\text{V}$ and $+15\text{V}$ indicators).
3. Obtain a 15-20 MHz *GPS stabilized* DDS clock signal (square wave) and connect it to the rear BNC input. This serves as the seed for the ADF4350 VCO.
4. Install the EVAL-ADF4350 interface software from Analog Devices' website and connect your PC to the rear USB port on the enclosure.
5. Obtain a (again, GPS stabilized, if possible) 80-130 MHz DDS clock signal (square wave) and connect it to the DDS REF input on the front of the box (the far right BNC connector, to the right of the dial). Other frequencies may work, but were not explicitly used during testing.
6. Using the Analog Devices software, set the ADF4350 unit to the appropriate frequency, **keeping in mind the frequency multipliers present in each FOL unit.** For example, for the ${}^6\text{Li}$ D1-D2 (10.056 GHz) unit, one would set the ADF4350 frequency to $(\nu_B - \nu_{DDS})/4$. **Do not forget to specify the seed clock frequency in the software**, that of the rear DDS input, or the VCO will not operate as intended.
7. Connect the SERVO output on the front of the enclosure to the laser PI servo unit. The SERVO output can be scaled using the knob next to it. The PHASE output is an unscaled duplicate of the SERVO output, and is to be used for monitoring with an oscilloscope.
8. Turn the proportional and integral gain of the laser PI servo off (two switches flipped to off position). Viewing the ROSA Monitor output on the spectrum analyzer. Use the coarse/fine adjustment knobs on the laser PI servo to get the laser beatnote to approximately the desired offset from the VCO carrier.
9. Turn the proportional, then integral, gains on. This may require ad-hoc tuning of the proportional/integral gains to achieve a stable lock. If the proportional gain is at a reasonable level, the beatnote, on the spectrum analyzer, should appear to be "smeared out" and jump around about the lock point (100-200 MHz away from the VCO carrier, whatever the FPD DDS REF is set to). Turning on the integral gain, at the correct level, removes this effect and should restore the beatnote to, or near, its original linewidth. If the integral gain is turned on and the lock is lost (the beatnote jumps outside the spectrum analyzer FOV), this means it is too high.

During closed loop testing of the ${}^6\text{Li}$ D1-D2 (10.056 GHz) unit, stable locking was achieved with $\nu_{DDS} = 120$ MHz. With proportional and integral gains set correctly, the linewidth of the beatnote was indistinguishable between open and closed loop operation, indicating that the FOL units have higher bandwidth than the laser PI servo itself.

NOTE: ROSA MONITOR and EVAL-ADF4350EB1Z OUT- SMA outputs **MUST** be terminated with 50Ω at all times to ensure correct operation (if not in active use, SMA-BNC adaptors and 50Ω BNC terminators are to be used).

NOTE: In the tested unit, the VCO signal couples weakly through the passive mixer back into the ROSA Monitor and is visibly superimposed on the beatnote spectrum when viewing the ROSA MONITOR output with a spectrum analyzer. This is useful for debugging. On the ROSA Monitor output, the VCO carrier is typically 15-25 dB lower than the beatnote amplitude on the spectrum analyzer.

NOTE: For the FOL units with frequency multiplier stages, the VCO carrier may be lower in power than the ROSA beatnote carrier. Because the RF/LO inputs of the passive mixers have different insertion/conversion losses it may help to swap the two inputs. The mixer, as placed in the enclosure, is shown here: and can simply be flipped upside down without having to change cable configurations.

C Signal Processing Block Diagrams

C.1 9200 – 11800 MHz Unit

C.2 3400 – 7800 MHz Unit

C.3 200 – 4400 MHz Unit

Summary

The Finisar HFD6180 LC ROSA photodetector unit is used internally to offset-lock a pair of lasers by detecting and transmitting a beat-note signal from the incident beams. Though the unit is advertised as a 10Gbps/5GHz receiver, it does have a specified -3dB high frequency cutoff at 9 ± 3 GHz. Questions were raised about its viability in the Li D1 offset range (10.4GHz). The unit has been tested previously and found to produce useable signals well above 10GHz, but no comprehensive data was ever collected or retained. Here, a pair of beams from the Ti:Sapphire laser are modulated and mixed : one fixed at ~ 630 THz and the other scanned at offsets between 0 - 15 Ghz. The power of the beat-note fundamental at the output of the ROSA unit was recorded over this range. For successful operation, the new locking circuit anticipates a minimum input from the ROSA of -40 dBm. In the 10.4 GHz regime, the output power of the ROSA unit as a function of incident beat-note power was found to saturate at approximately -27.5 dBm. Its performance in locking electronics will be heavily dependent on incident beam power, as well as operating frequency.

Methodology

Using the Agilent E4407B (26.2 GHz) spectrum analyzer, the fundamental beat-note power was measured at the SMA output of the ROSA unit. The power of each constituent laser beam was measured with a power-meter, (beams were isolated by blocking one or the other with a thick paper card). Beams were coupled into a fiber splitter with one feeding the ROSA unit and the other end going to a power-meter or wav-ometer as necessary. It is useful to understand the power transfer as a function of incident beam power, so as to know minimum requirements for a particular setup. For these measurements. two beams were locked at ~ 10.4 GHz and their input power was varied by manipulating the fiber coupling optics, (not the laser cavities). There are a few specific points with mentioning about the measurements:

- The coupling through the fiber splitter is not the same for both beams/destinations. There are 4 different coupling ratios from sources to destinations, which should remain the same if the fiber coupling itself is unchanged. These ratios were measured once at the start and end of the experiment and the data shown here is corrected accordingly.
- A particular configuration was considered mode-stable if the beat-note fundamental, as seen by the spectrum analyzer, was the only significant feature. Realistically there could be multiple side-bands present during every measurement, but any side-bands under -40 dBc were considered negligible and were ignored, (this is the condition for measurement consistency).
- The same power-meter was used for all power measurements. Furthermore, the spectrum analyzer was set to an attenuation of 0dB with a reference level of -10dB. To reduce sampling error, the bandwidth of the sweep was kept to within 1GHz of the beatnote fundamental.

The incident power of the beat-note as a function of the intensity of the two beams is obtained the usual way, (integrate the Poynting vector over one period and divide by the same period, assuming monochromatic light):

$$P_{beat} \propto |Ae^{i\omega_1 t} + Be^{i\omega_2 t}|^2 = A^2 + B^2 + 2AB \cos((\omega_1 - \omega_2)t) \quad (1)$$

$$P_{ROSA} = I_{ROSA}^2 \cdot R = I_{ROSA}^2 \cdot 50 \quad | \quad I_{ROSA} \propto P_{beat} \quad (2)$$

$$P_{ROSA} = (\alpha 2AB)^2 \cdot R \quad \rightarrow \quad \log |P_{ROSA}| = 2 \log |A| + 2 \log |B| + 2 \log |2\alpha| + \log |50| \quad (3)$$

Where α is some parameter that defines the power transfer, and P,A,B are power, in watts. Presumably, α encapsulates both the *spectral responsivity* of the photodiode and the power transfer of the transimpedance amplifier present in HFD6180. The assumed current-incident power relationship is linear in the nonsaturation regime, as stated in (2). Presumably, the output power of the ROSA unit as a function of input Beam power should match the form of (3), with α to be determined.

Results / Discussion

Using the Agilent E4407B (26.2 GHz) spectrum analyzer, the fundamental beat-note power was measured at the SMA output of the ROSA unit. The power of each constituent laser beam was measured with a power-meter, (beams were isolated by blocking one or the other with a thick paper card). The error of the spectrum analyzer measurements was consistently in the ± 0.1 dBm range, and is ignored here. Similarly, the incident laser beams were stable to within 5% of mean power and this variation is also ignored. The laser unit had a scanning bandwidth of around 10GHz and it was necessary to scan through two modes to obtain the results shown in **Figure 1**.

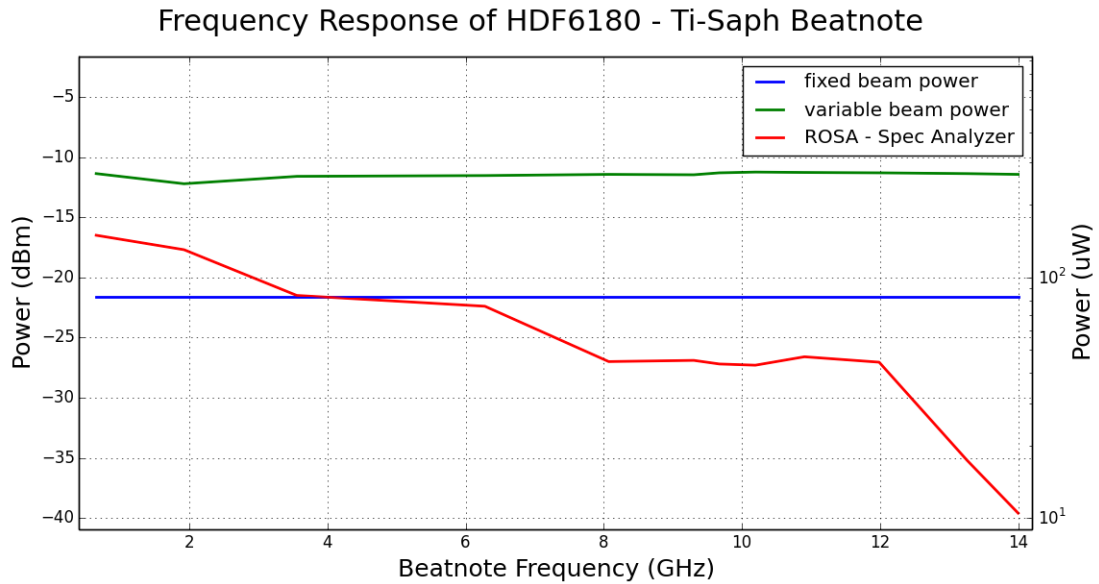


Figure 1: Input beam/ and output signal power, pre and post ROSA unit.

Occasionally, during scanning, some side-bands were observed, with amplitudes as high as -5 dBc to -10 dBc (approximately 50-30% of the carrier power). Ideally, the lasers would be mode-stable during experiments and not exhibit the frequency mode hopping that was sometimes observed. All reported measurements are averages of several samples (usually 5-10), and so the effect of these side bands is somewhat minimized.

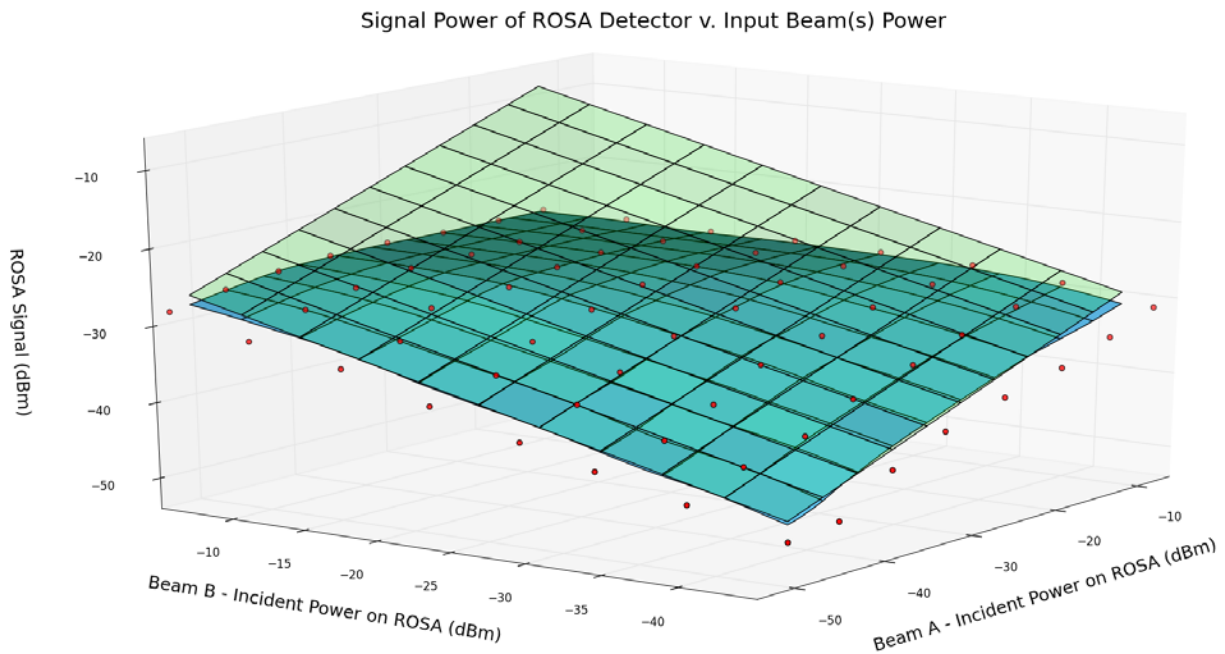


Figure 2: Power transfer results, shown in 3D for qualitative understanding, with the physical measurements shown as red dots. The interpolant, shown in blue, was used to generate the reference data in **Table 1**. The least squares fit for the presumed linear region, in transparent green, is for comparing the data to the form of (3).

The blue interpolant from **Figure 3** was sampled at some reference values to provide a convenient look-up table for experimental use (**Table 1**). Half the table could be thought to be redundant, but there is a slight variation. As the table is generated automatically by a script, the values are included for reference.

Table 1: Lookup table for matching input beam powers (in uW and dBm) to ROSA signal output power (dBm only). Numerical values below are from interpolant shown in **Figure 3**

		Beam A										
		(dBm)	-40.00	-36.67	-33.33	-30.00	-26.67	-23.33	-20.00	-16.67	-13.33	-10.00
Beam B		(dBm)	10.00	14.68	21.54	31.62	46.42	68.13	100.00	146.78	215.44	316.23
-40.00	10.00	-42.87	-41.18	-39.52	-37.80	-36.29	-35.06	-33.72	-32.48	-31.26	-30.38	
-36.67	14.68	-41.55	-39.97	-38.20	-36.28	-34.76	-33.61	-32.52	-31.34	-30.25	-29.49	
-33.33	21.54	-39.56	-38.07	-36.66	-34.82	-33.28	-32.12	-31.10	-30.08	-29.18	-28.71	
-30.00	31.62	-37.90	-36.58	-35.28	-33.51	-32.05	-30.95	-30.01	-29.15	-28.49	-28.17	
-26.67	46.42	-36.32	-34.99	-33.73	-32.03	-30.67	-29.82	-29.13	-28.49	-28.01	-27.87	
-23.33	68.13	-34.74	-33.47	-32.18	-30.71	-29.49	-28.87	-28.43	-28.03	-27.79	-27.73	
-20.00	100.00	-33.28	-32.09	-30.90	-29.60	-28.69	-28.23	-28.02	-27.83	-27.70	-27.68	
-16.67	146.78	-31.72	-30.68	-29.73	-28.80	-28.13	-27.88	-27.79	-27.70	-27.62	-27.62	
-13.33	215.44	-30.59	-29.68	-28.93	-28.25	-27.85	-27.71	-27.68	-27.63	-27.59	-27.58	
-10.00	316.23	-29.62	-28.88	-28.29	-27.83	-27.65	-27.55	-27.57	-27.60	-27.60	-27.59	

A rather surprising result from this test is that the data in the nonsaturation region does not seem to follow the form of (3). The plane equation determined by the least squares solver for the data in the nonsaturation region is:

$$Z = 0.473 \cdot X + 0.466 \cdot Y - 5.438 \quad (4)$$

For the fitting, all data was in units of dBm. Stating (3) with original measurement units:

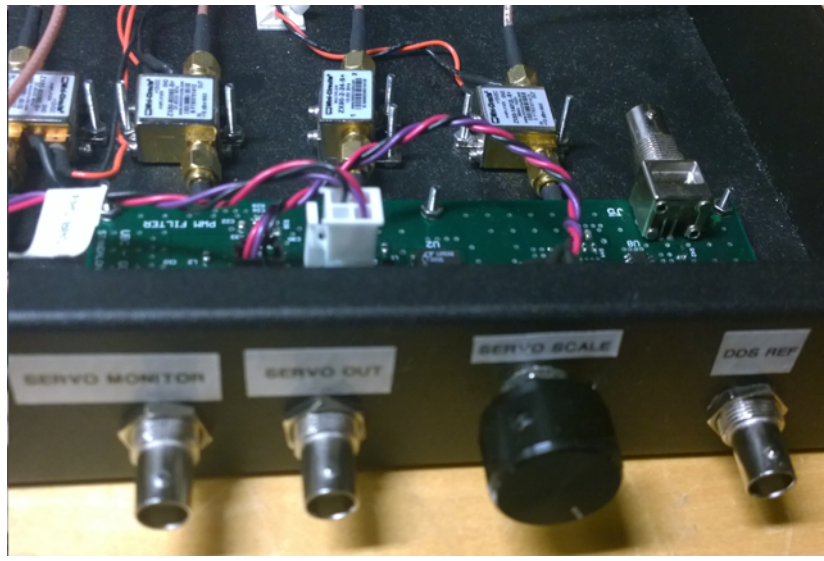
$$P = 0.473 \cdot \log_{10} |A^2 * 1000| + 0.466 \cdot \log_{10} |B^2 * 1000| - 5.438$$

$$\therefore P = 0.946 \log_{10} |A| + 0.932 \log_{10} |B| - 2.620$$

Where P is in dBm and A^2, B^2 are in μW . Note that the plotted points are the measured power in dBm which is proportional to the square of the intensities, A, B. This gives a value of $6.57 \text{ mA}/\mu W$ for α , which sounds reasonable. However, the validity of this model is called into question given that the slope of the plane in each dimension is far from 2, as stated in (3). In fact, the plane fitted to the data seems to suggest that $P_{ROSA} \propto (AB)$, and it is not apparent why this should be.

Conclusion

The locking circuit for the Li D1 system, which is to be extended to the Rb85/87 systems in the future, was designed with a minimum input power requirement of -40 dBm. For a 10GHz input, the HFD6180 was shown to output a ~ -30 dBm signal. The HFD6180 will be retained for use in the D1 locking electronics, and extended to the Rb87/85 locking electronics as well. Usage in regimes higher than 12-14 GHz, and below an input beam power of -35 dBm ($17.8 \mu W$) is not recommended without significant amplification. Linear relationships between incident and output power, even below the measured saturation limit, should not be assumed.



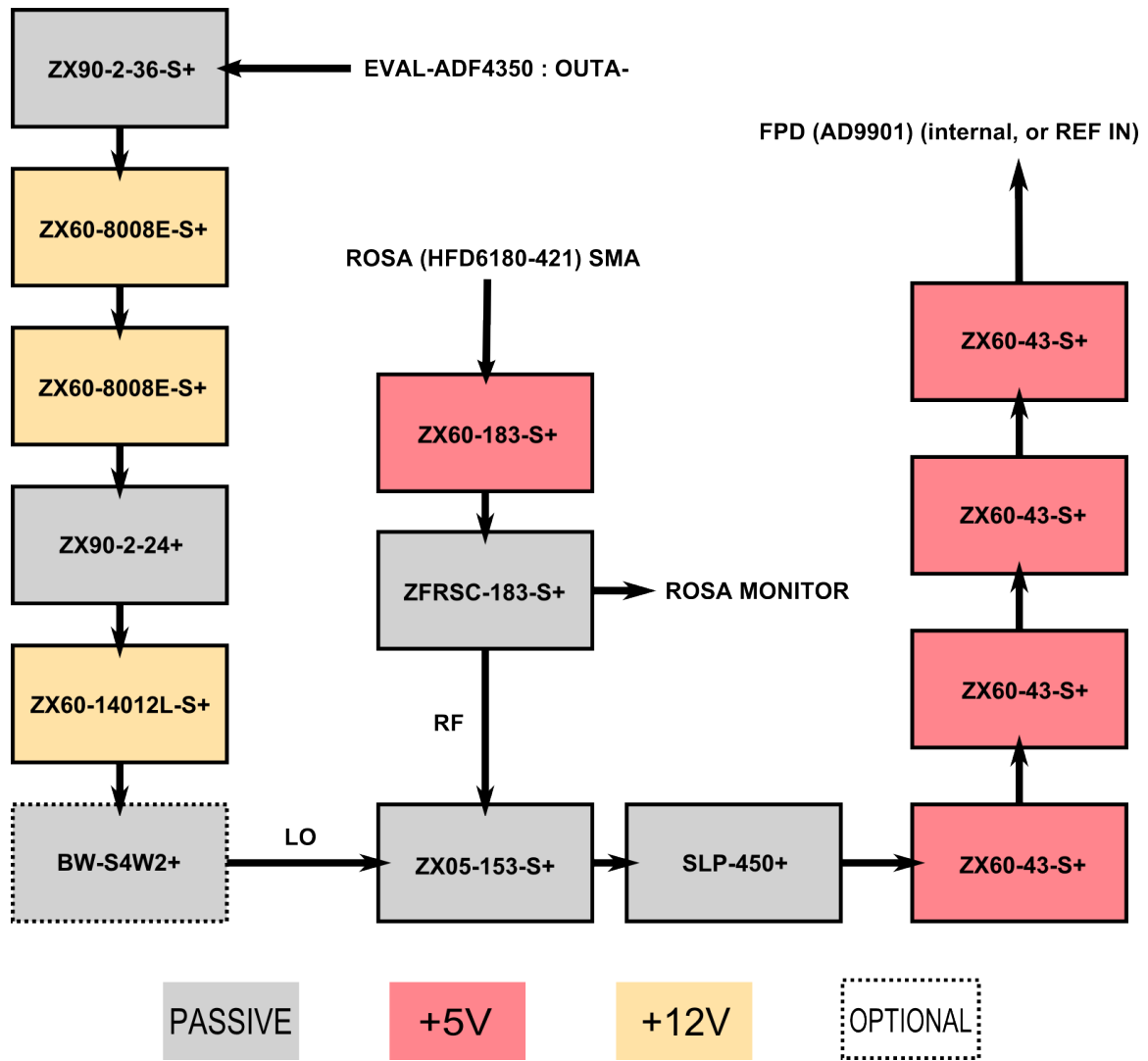


Figure 15: Signal processing pipeline for ${}^6\text{Li}$ D1-D2 (10.056 GHz) error signal.

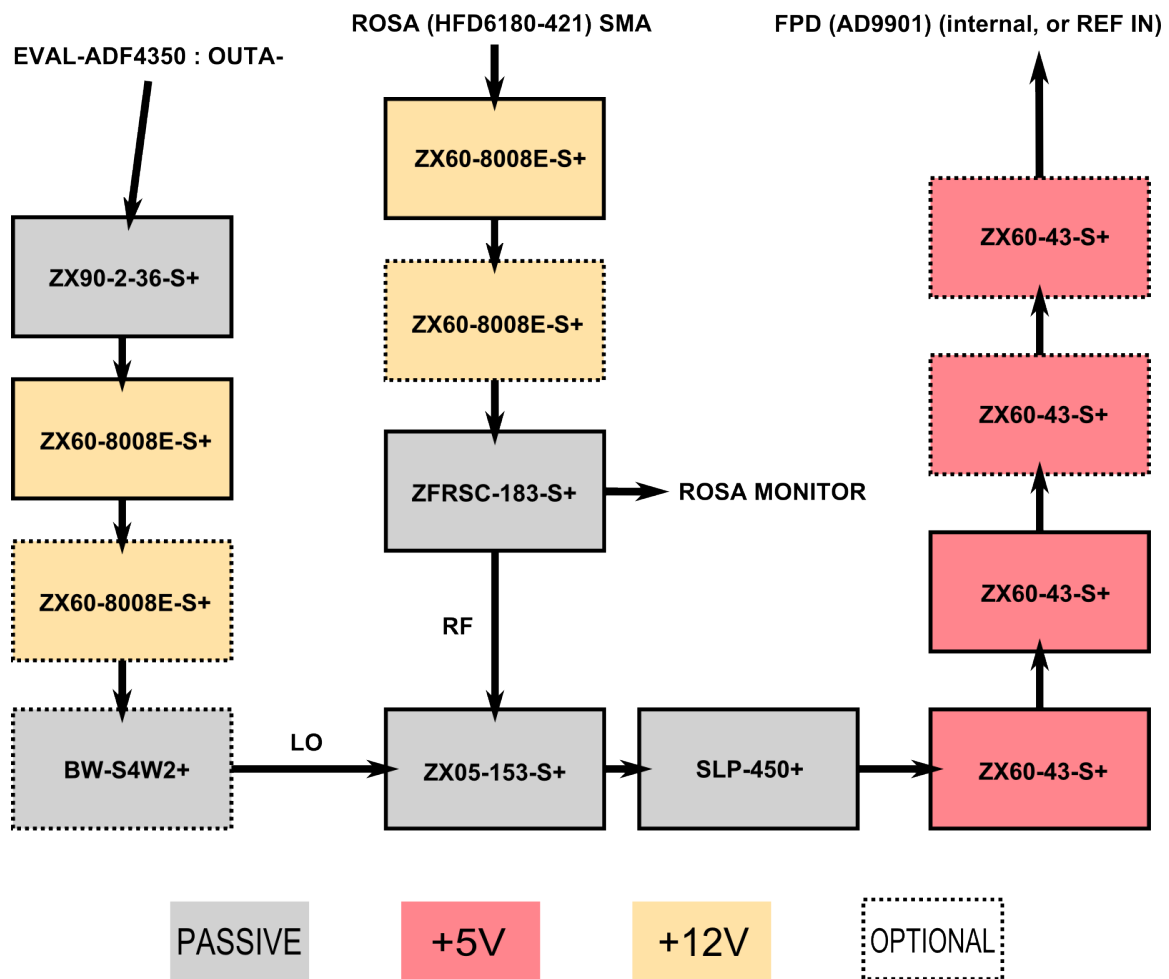


Figure 16: Signal processing pipeline for ^{87}Rb D2 pump/repump (6.568 GHz) error signal.

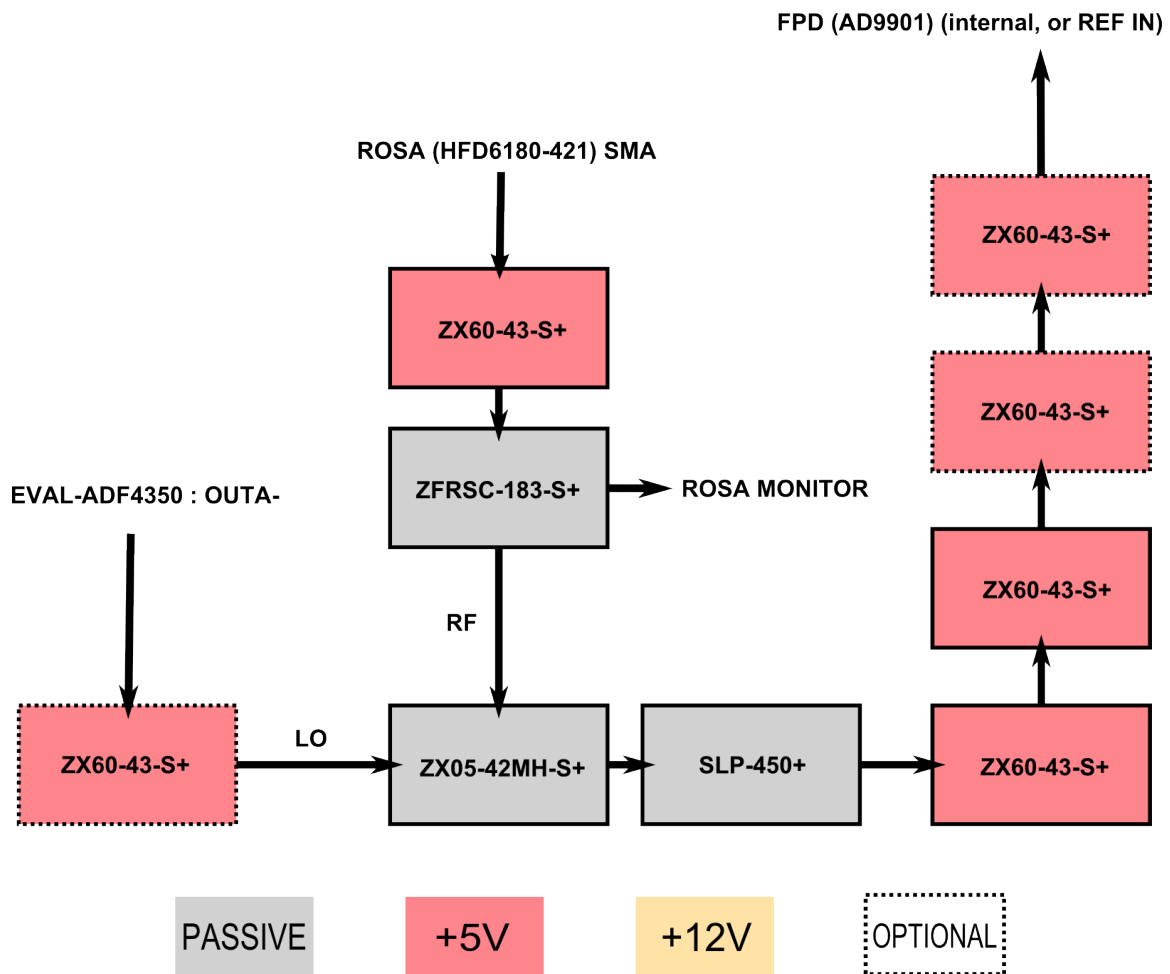


Figure 17: Signal processing pipeline for ^{85}Rb D2 pump/repump (2.915 GHz) error signal. Due to this FOL unit's bandwidth being outside of the passband of ZX05-153-S+, it was changed to ZX05-42HM-S+.